PROCEEDINGS, 49th Workshop on Geothermal Reservoir Engineering
Stanford University, Stanford, California, February 12-14, 2024
SGP-TR-227

The Updated Wellbore Stress Models for Utah FORGE

Zhi Ye[1,2] and Ahmad Ghassemi[1]

1. Reservoir Geomechanics and Seismicity Research Group, The University of Oklahoma, Norman, OK 73069

2. Now at Department of Geology and Geological Engineering, South Dakota Mines, Rapid City, SD 57701

ahmad.ghassemi@ou.edu

Keywords: FORGE, In-situ Stress, Wellbore Failure, Image Logs, Drilling-induced Fractures, Stress Inversion

ABSTRACT

A significant issue in the planned research and development (R&D) activities at Utah FORGE is the characterization of the in-situ stress. Previously, we reported constrained wellbore stress models for three vertical wells at FORGE: 58-32, 56-32, and 78B-32 (Ye et al., 2022; Fang et al., 2022). In this paper, we present the updated wellbore stress models for Utah FORGE, focusing on the deviated well: 16A(78)-32. To determine the maximum horizontal stress (S_{Hmax}), we integrated the drilling-induced fractures and the transverse fractures observed within the borehole image logs. We applied two methods: Method 1 directly solves the equation systems with S_{Hmax} as the only unknown parameter, while Method 2 uses a stress inversion technique to obtain the inversion results of three unknown parameters: the magnitudes of S_{Hmax}, the orientation of S_{Hmax}, and the fracture trace angle (ω). Method 2 appears to provide more reliable stress results, suggesting that the constrained S_{Hmax} ranges from 0.81-1.06 psi/ft indicating a normal to potentially transitional normal-strike-slip faulting regime. On the other hand, Method 1 provides scattered results, showing the magnitude of S_{Hmax} is about 0.88-1.37 psi/ft, suggesting the existence of possible strike-slip faulting in deep formations. Furthermore, the orientation of S_{Hmax} obtained from Method 2 ranges from N5E to N30E. This is consistent with the stress orientation indicated by drilling-induced fractures observed from the image logs. Our results also reveal the presence of thermally induced transverse fractures, though most transverse fractures could still be natural in origin.

1. INTRODUCTION

Reliable knowledge of the magnitudes and orientations of in-situ stress is essential for conducting scientific and engineering activities in the subsurface, especially with regards to subsurface energy and storage applications. Specifically, in the context of Enhanced Geothermal Systems (EGS) development, understanding these stresses is fundamental for effective reservoir characterization, the optimization of drilling operations, the efficiency of hydraulic stimulation processes, and the mitigation of induced seismic activities. To accurately characterize in-situ stress, it is necessary to determine six independent components of the stress tensor: the magnitudes of the three principal stresses along with their orientations. In the upper layers of the Earth's crust, these principal stresses typically include the vertical stress (S_v), the minimum horizontal stress (S_{hmin}), and the maximum horizontal stress (S_{Hmax}). The vertical stress (S_v) is generally calculated from the density log data. The minimum horizontal stress can be fairly determined through hydraulic fracturing (HF)-based on techniques, such as DFIT, leak-off tests, and microfrac tests. Additionally, techniques such as the analysis of wellbore failures, cross-dipole sonic logs, and seismic focal mechanisms can be utilized to determine the orientations of horizontal stresses. Nonetheless, determining the maximum horizontal principal stress (S_{Hmax}) remains a complex challenge. Traditional methods, which often infer S_{Hmax} from hydraulic fracturing data using elasticity theory, face significant uncertainties (Zoback and Haimson, 1982; Schmitt and Zoback, 1989). These uncertainties have prompted the development of more reliable techniques based on the analysis of borehole breakouts and drilling-induced tensile fractures observed in borehole image logs, offering a more accurate estimation of S_{Hmax} (for example, see Bell and Gough, 1983; Brudy & Zoback, 1998).

The Frontier Observatory for Research in Geothermal Energy (FORGE), an initiative funded by the U.S. Department of Energy (DOE), is dedicated to creating a full-scale Enhanced Geothermal Systems (EGS) laboratory near Milford, Utah (Moore et al., 2020). One of FORGE's pivotal research focuses is the accurate determination of in-situ stress, a topic that has gained substantial interest due to its crucial role in developing a successful EGS within granitoid formations deeper than 8,500 feet below the surface. At the Utah FORGE site, a pair of injection-production wells have been directionally drilled at a 65° inclination to the vertical (16A(78)-32 and 16B(78)-32). In addition, several monitoring wells have been drilled, including the deep vertical wells of 58-32, 56-32, and 78B-32. Utilizing advanced borehole imaging techniques, such as the Formation Micro Imager (FMI) and Ultrasonic Borehole Imager (UBI), the project has identified numerous drilling-induced fractures (DIFs) and some borehole breakouts in both the vertical monitoring wells and the deviated injection well. These observations from borehole image logs are instrumental in defining the in-situ stress field, particularly in estimating the maximum horizontal stress (S_{Hmax}), which is crucial for the design and optimization of the EGS at this depth.

In previous work, we conducted stress analysis on three vertical wells (58-32, 56-32, and 78B-32). This was based on borehole failure observations from image logs and led to the establishment of a stress profile for these wells (Ye et al., 2022; Fang et al., 2022). This paper expands on that foundation by introducing updated wellbore stress models for the deviated injection well, 16A(78)-32. Notably, this well exhibited hundreds of drilling-induced fractures (DIFs), indicative of tensile failures surrounding the wellbore. The analysis of a deviated well like 16A(78)-32 presents more complexity than vertical wells due to the misalignment of wellbore coordinates with principal stress orientations, requiring an advanced approach to stress analysis. To assess the stress around the deviated well 16A(78)-32, we initially correlated wellbore stress with in-situ stress via stress rotation, thereby identifying the principal stresses around the wellbore and establishing a criterion for drilling-induced tensile fractures. Our methodology encompasses two approaches for constraining the

maximum horizontal stress (S_{Hmax}): the first (Method 1) directly calculates S_{Hmax} as the sole unknown, and the second (Method 2) employs a stress inversion technique to deduce three unknowns— the magnitudes of S_{Hmax}, the orientation of S_{Hmax}, and the fracture trace angle (ω). Additionally, we observed numerous closely spaced, non-continuous transverse fractures at the bottom section of the injection well, likely resulting from thermally induced tensile stresses due to cooling from the drilling mud or from pre-existing natural fractures. We further analyzed these transverse fractures to ascertain their origins, offering supplementary constraints for S_{Hmax}'s determination. The updated stress models for well 16A(78)-32 aim to enhance the accuracy of in-situ stress estimations at the Utah FORGE site, supporting the broader goals of stress determination in conjunction with other research activities.

2. STRESS AROUND THE WELLBORE WALL OF AN ARBITRARILY ORIENTATED BOREHOLE

Unlike vertical wells where the wellbore trace is aligned with the vertical stress orientation, an arbitrarily oriented borehole presents a more complex scenario. In such cases, the wellbore stress coordinates and the in-situ stress coordinates may orient in various directions. This divergence in alignment necessitates a nuanced approach for stress rotation and analysis, as the direct correlation between wellbore orientation and principal stress directions, evident in vertical wells, does not exist in deviated or arbitrarily oriented boreholes. We use three Cartesian coordinate systems to describe the stress state on the borehole wall. As shown in Figure 1, the geographical coordinate system, which utilizes a North-East-Down (NED) orientation, is employed to bridge the in-situ stress coordinate system with that of the wellbore coordinate system. The geographical system aligns the in-situ stress directions relative to the Earth's surface (North-East-Down), which is crucial for accurately correlating the orientations and measurements between the in-situ stresses and the wellbore trajectories in stress analyses (e.g., Peska & Zoback, 1995; Okabe et al., 1998; Huang et al., 2011).

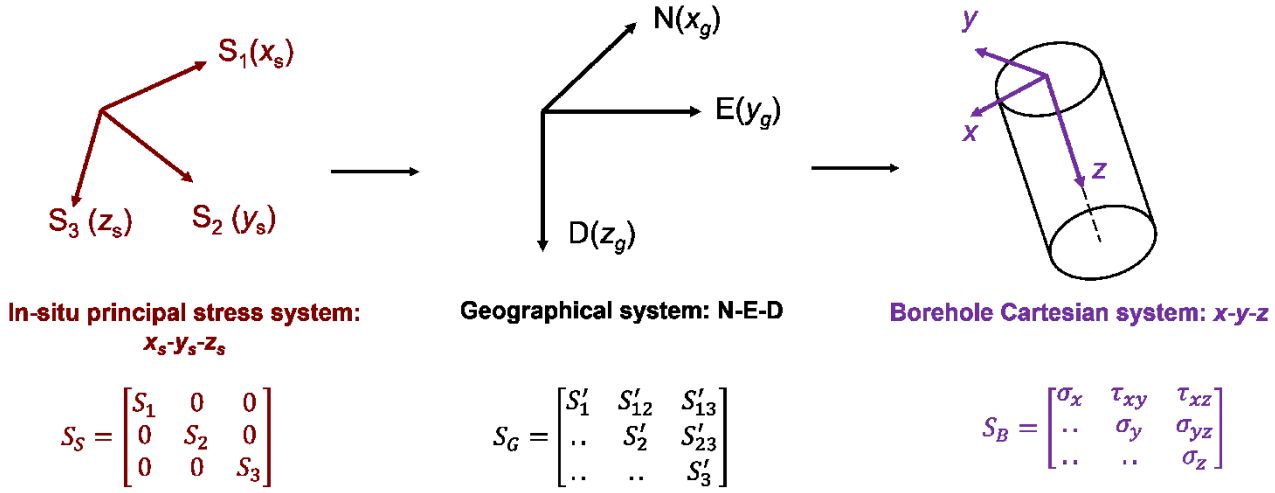

Figure 1: There are three Cartesian coordinate systems used to describe the stress state on the borehole wall: the in-situ principal stress system, the geographical system, and the local borehole Cartesian system. The borehole Cartesian system adheres to the right-handed rule. The *z*-axis lies along the borehole trace (down is positive), while the *x*-axis and *y*-axis are oriented horizontally in the plane perpendicular to the hole axis. The *x*-axis points to the bottom side of the borehole. Three stress tensors—S_S, S_G, and S_B—represent the stress state within these three Cartesian coordinate systems, respectively.

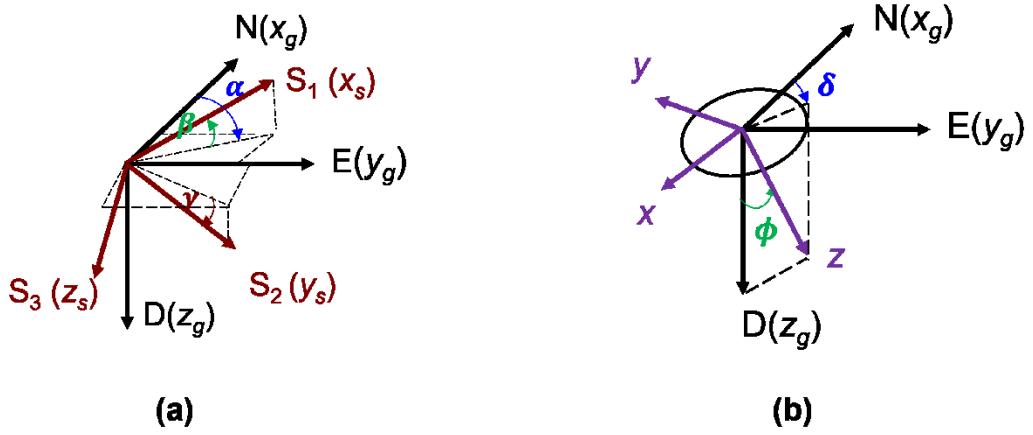

Figure 2: (a) The rotation from the geographical coordinate system to the in-situ stress coordinate system; (b) the rotation from the geographical coordinate system to the local borehole Cartesian coordinate system.

The geographical coordinate system serves as a pivotal link between the in-situ stress coordinate system and the local borehole coordinate system, both of which can have arbitrary orientations. As depicted in Figure 2(a), the transition from the geographical coordinate system to the in-situ stress system is executed through a series of three rotations, defined by Euler angles α, β, and γ. Consequently, the in-situ principal stress can be shifted to the geographical coordinate system based on this stress rotation:

$$S_G = R_{GP}^T S_p R_{GP} \tag{1}$$

$$R_{GP} = \begin{bmatrix} cos\alpha cos\beta & sin\alpha cos\beta & -sin\beta \\ cos\alpha sin\beta sin\gamma - sin\alpha cos\gamma & sin\alpha sin\beta sin\gamma + cos\alpha cos\gamma & cos\beta sin\gamma \\ cos\alpha sin\beta cos\gamma + sin\alpha sin\gamma & sin\alpha sin\beta cos\gamma - cos\alpha sin\gamma & cos\beta cos\gamma \end{bmatrix} \tag{2}$$

Where R_{GP} is the rotation matrix for rotating the geographical coordinate system to the in-situ stress coordinate system. The Euler angles α, β, and γ are connected to the orientations of the in-situ stresses.

Additionally, the borehole's geometry can be characterized using two angles: δ, the azimuth of the borehole's horizontal projection, measured clockwise from north to east, and ϕ, the deviation angle from the vertical axis. As depicted in Figure 2(b), the rotation from the geographical coordinate system to the local borehole system is governed by the angles δ and ϕ. As a result, the stress rotation allows the wellbore stress tensor to be represented in the geographical coordinate system.

$$S_B = R_{GB} S_G R_{GB}^T \tag{3}$$

$$R_{GB} = \begin{bmatrix} -cos\phi cos\delta & -cos\phi sin\delta & sin\phi \\ sin\delta & -cos\delta & 0 \\ sin\phi cos\delta & sin\phi sin\delta & cos\phi \end{bmatrix} \tag{4}$$

Where R_{GB} is the rotation matrix for rotating the geographical coordinate system to the local wellbore coordinate system.

According to the above two-steps stress rotation, the wellbore stress tensor can be linked to the in-situ stress tensor and described as:

$$S_B = R_{GB}(R_{GP}^T S_S R_{GP}) R_{GB}^T \tag{5}$$

Moreover, the stress acting on the borehole wall in the Cartesian coordinate system can be represented in the cylindrical coordinate system using Kirsch's solution (Aadnary & Chenevert, 1987). This assumes that the rock is isotropic, homogeneous, and a linearly elastic material. The thermal stress resulting from wellbore cooling can also be factored into the stress analysis. Therefore, the stresses at borehole wall in the cylindrical system are as follows:

$$\sigma_{rr} = P_w \tag{6}$$

$$\sigma_{\theta\theta} = \sigma_x + \sigma_y - 2(\sigma_x - \sigma_y)\cos 2\theta - 4\tau_{xy}\sin 2\theta - P_w + \frac{\alpha_T E \Delta T}{1-2\nu} \tag{7}$$

$$\sigma_{zz} = \sigma_z - 2\upsilon(\sigma_x - \sigma_y)cos2\theta - 4\upsilon\tau_{xy}\sin 2\theta + \frac{\alpha_T E \Delta T}{1-2\nu} \tag{8}$$

$$\tau_{r\theta} = \tau_{\theta r} = 0 \tag{9}$$

$$\tau_{\theta z} = \tau_{z\theta} = 2(-\tau_{xz}\sin\theta + \tau_{yz}\cos\theta) \tag{10}$$

$$\tau_{rz} = \tau_{zr} = 0 \tag{11}$$

Where σ_{rr}, $\sigma_{\theta\theta}$, σ_{zz}, $\tau_{r\theta}$, $\tau_{\theta z}$, and τ_{rz} are the stress components of borehole stress tensor in the cylindrical coordinate system; σ_x, σ_y, σ_z, τ_{xy}, τ_{xz}, and τ_{yz} are the stress components of borehole stress tensor in the Cartesian coordinate system; θ is the circumferential angle measured clockwise starting from the *x*-axis. It can be inferred from image logs for an individual borehole failure, such as a drilling-induced fracture, a breakout, or a transverse fracture; the P_w is the wellbore pressure; υ is the Poisson's ratio; α_T is the thermal expansion coefficient; E is the Young's modulus; ΔT is the temperature difference due to cooling.

The three primary stresses at the borehole wall can then be determined as follows:

$$\sigma_{rr} = P_w \tag{12}$$

$$\sigma_{tmax} = \frac{1}{2}\left[\sigma_{\theta\theta} + \sigma_{zz} + \sqrt{(\sigma_{\theta\theta} - \sigma_{zz})^2 + 4{\tau_{\theta z}}^2}\right] \tag{13}$$

$$\sigma_{tmin} = \frac{1}{2}\left[\sigma_{\theta\theta} + \sigma_{zz} - \sqrt{(\sigma_{\theta\theta} - \sigma_{zz})^2 + 4{\tau_{\theta z}}^2}\right] \tag{14}$$

Where σ_{tmax} and σ_{tmin} are the maximum and minimum principal stresses in the plane tangential to the borehole.

Therefore, the criteria for tensile failure (drilling-induced fractures) and compressive failure (borehole breakouts) at the borehole wall can be described as follows:

$$\sigma_{tmin} - \alpha P_p = -T \tag{15}$$

$$\sigma_{tmax} - \alpha P_p = C_0 \tag{16}$$

Where P_p is the pore pressure; α is the Biot's coefficient, it is set to 1 in this study; T is the rock's tensile strength; C_0 is the rock's compressive strength.

3. STRESS DETERMINATION THROUGH THE DRILLING-INDUCED FRACTURES

In the deviated well 16A(78)-32, borehole image logs have revealed roughly 400 drilling-induced fractures (DIFs), indicating tensile failures along the wellbore wall. These fractures provide critical data for borehole stress analysis, as detailed in Section 2. This analysis facilitates the estimation of the maximum horizontal stress (S_{Hmax}) by using additional data on the vertical stress (S_v), the minimum horizontal stress (S_{hmin}), the pore pressure (P_p), the wellbore pressure (P_w), and rock properties. The deviated well is composed of three distinct sections: a vertical section, a build-up or dogleg section, and a hold section. The build-up section's pronounced curvature may compromise the image log quality due to the possible stick-slip interactions between the logging tool and the curved wellbore wall. Consequently, for the purposes of stress analysis, only the DIFs identified in the vertical and hold sections were considered, while the image logs from the build-up section were excluded.

To determine the magnitude of S_{Hmax}, we applied two distinct methodologies. Method 1 involved solving a single equation (Equation 15 from Section 2), where S_{Hmax} was set to be the only unknown parameter. In contrast, Method 2 implemented a stress inversion technique that yields results for three unknown parameters: the magnitudes of S_{Hmax}, the orientation of S_{Hmax}, and the angle of fracture trace. This dual-method approach enhanced the reliability and comprehensiveness of our stress determination in well 16A(78)-32.

3.1 Method 1

In Method 1, we utilized Equation 15 as the primary equation for determining the magnitude of S_{Hmax}, which is inferred from the tensile failures around the wellbore, as evidenced by the drilling-induced fractures (DIFs) observed. This equation establishes a connection with the in-situ stresses, aligning with Equations 1-11 and 14. For this analysis, all parameters, except for the magnitude of S_{Hmax}, are known and outlined in Table 1. These parameters are derived either directly or indirectly from a variety of field tests and laboratory experiments, such as borehole image logs, minifrac tests, and uniaxial as well as triaxial compression tests. Notably, the orientation of S_{Hmax} is assumed to be an average value of N25°E. This is based on the azimuth range of N10°E to N40°E observed in the drilling-induced fractures from the image logs of the injection well 16A(78)-32 (see Figure 5(b)). The significance of this orientation lies in its role in determining the α angle within the rotation matrix R_{GP}, as detailed in Equation 2.

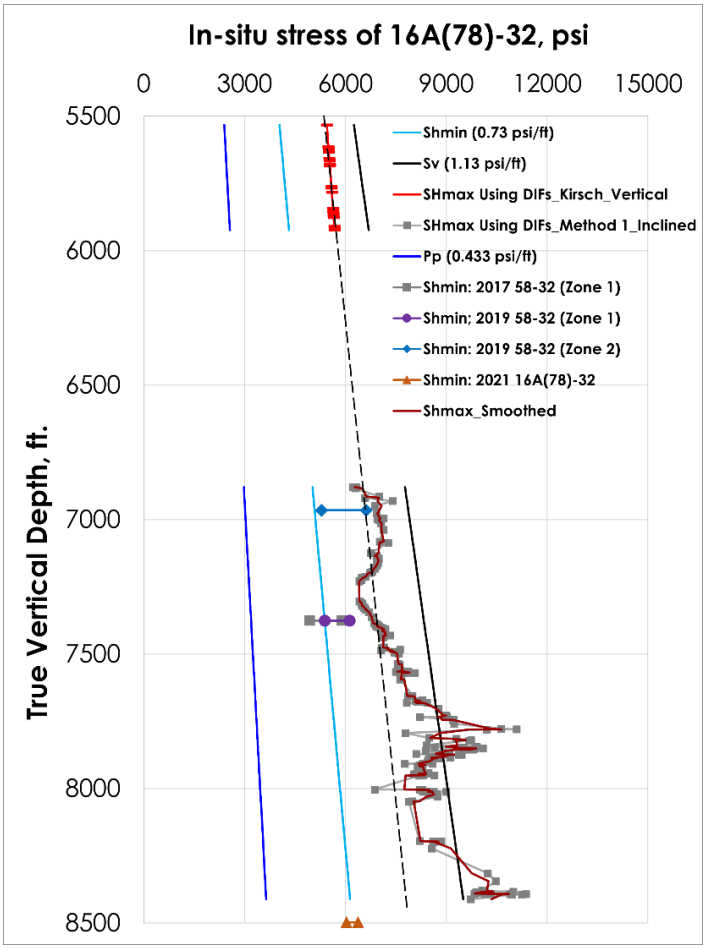

Figure 3: The stress profile of the deviated well 16A(78)-32 using Method 1.

Table 1: Input parameters used for constraining the maximum horizontal stress (S_{Hmax}).

Parameter	Value	Description	Source
S_v	1.13 psi/ft	Vertical Stress	(Moore et al., 2020)
S_{hmin}	0.73 psi/ft	Minimum horizontal stress	DFIT test 0f 16A(78)-32 (Xing et al., 2021)
P_p	0.433 psi/ft	Pore pressure	(Moore et al., 2020)
ρ_m	9 ppg	Mud weight	Drilling report of 16A(78)-32
E	7910000 psi	Young's modulus	Average values from the laboratory core tests (McLennan, 2018)
ν	0.29	Poisson ratio	
T	1605 psi	Tensile strength	
α_T	0.000004 1/K°	Thermal expansion coefficient	Inferred from lab test (Zhou & Ghassemi, 2023)
ΔT	50-60 C°	Temperature difference due to cooling	Drilling & Logging Report of 16A(78)-32
*S_{Hmax}'s orientation	N25E	The orientation of S_{Hmax}	Borehole Image logs of 16A(78)-32

* In Method 1, the orientation of S_{Hmax} is required as an input parameter. Conversely, for Method 2, it is not required and is set as an unknown parameter.

Figure 3 presents the stress profile for well 16A(78)-32, as determined using Method 1. This profile specifically showcases the stress results from the vertical section (spanning 5,500 to 5,900 feet) and the hold section (ranging from 6,800 to 8,400 feet). Notably, the build-up section, which lies between 5,900 and 6,800 feet, is excluded from this analysis due to the uncertainties associated with its curvature. Within the vertical section, the magnitude of S_{Hmax} ranges between 0.96 and 0.98 psi/ft. Conversely, in the hold section, S_{Hmax}'s magnitude appears more variable, ranging from 0.88 to 1.37 psi/ft. This variability suggests the potential presence of strike-slip faulting in the deeper formations, as inferred from the stress data. The process of conducting stress analysis in a deviated well like 16A(78)-32 is significantly influenced by complex stress rotations and the precise measurement of individual drilling-induced fractures. Consequently, the results are sensitive to some of input parameters, such as the α angle within the rotation matrix R_{GP}(Equation 2), which is related to the orientation of S_{Hmax}. Given that Method 1 relies solely on one equation to constrain S_{Hmax}'s magnitude, this might contribute to the observed scatter in the stress results.

3.2 Method 2

In Method 2, additional constraints are introduced for a more accurate determination of S_{Hmax}'s magnitude, employing two supplementary equations. This method is predicated on the premise that tensile failures manifest at positions around the wellbore wall where σ_{tmin} (Equation 15) reaches extremum values (e.g., Okabe et al., 1998; Huang et al., 2011). Therefore, the differentiation of σ_{tmin} with respect to the circumferential angle θ is set to zero.

$$\frac{\partial \sigma_{tmin}}{\partial \theta} = 0 \tag{17}$$

Additionally, as demonstrated in Equations 12-14, σ_{rr} is one of principal stress, while σ_{tmax} and σ_{tmin} represent another two principal stresses in the plane tangential to the borehole. Thus, the fracture trace angle ω should meet the following condition to vanish shear stress components in the principal stress tensor at the borehole wall (e.g., Aadnoy, 1990; Thorsen, 2011):

$$\tan(2\omega) = \frac{2\tau_{\theta z}}{\sigma_{zz} - \sigma_{\theta\theta}} \tag{18}$$

Unlike Method 1, which considers only the magnitude of S_{Hmax} as the unknown, Method 2 expands the analysis by introducing three unknown parameters: the magnitude of S_{Hmax}, the orientation of S_{Hmax} (related to the α angle in the rotation matrix R_{GP}), and the fracture trace angle (ω). This method uses known parameters such as vertical stress (S_v), minimum horizontal stress (S_{hmin}), pore pressure (P_p), wellbore pressure (P_w), and the properties of the surrounding rock (see Table 1). It applies three nonlinear equations—Equations (15), (17), and (18)—for a simultaneous solution through the Newton-Raphson method for enhanced precision.

Figure 4 presents the stress profile for the deviated well 16A(78)-32, where S_{Hmax}'s magnitude has been refined using Method 2. This approach yields a more consistent range of S_{Hmax} values compared to those derived from Method 1, particularly in the hold section, where S_{Hmax} varies from 0.81 to 1.06 psi/ft. This range aligns more closely with the values observed in the vertical section, indicating a reduction in variability and an improvement in the accuracy of stress estimation. The analysis suggests that the formation encountered during the drilling of well 16A(78)-32 is predominantly under a normal faulting regime. This is also in line with the stress results established from the three previously vertical wells.

Additionally, Figure 5(a) illustrates the orientation of S_{Hmax} as deduced from the α angle in the rotation matrix R_{GP}, determined using Method 2. This inferred orientation of S_{Hmax} ranges from N5°E to N30°E, averaging at N15°E. Notably, this range aligns with the orientation of S_{Hmax} observed in the drilling-induced fractures from the image logs of the injection well 16A(78)-32, as shown in Figure 5(b), which spans from N10°E to N40°E with an average of N25°E. The orientation inferred through Method 2 demonstrates a more focused distribution, likely offering a higher degree of reliability. This enhancement in precision is attributed to the constraints imposed by the three equations employed in Method 2, along with the automatic exclusion of any non-converging results, thereby refining the accuracy of the orientation determination.

Method 2, which encompasses the use of Equation 18, offers the capability to estimate the fracture trace angle. This angle is defined as the one formed between the trace of the fracture and the axis of the wellbore (Peška & Zoback 1995, Aadnoy & Bell 1998). In this context, the convention is to measure the fracture trace angle as positive when it is oriented clockwise from the wellbore axis towards the fracture trace when looking outwards from the wellbore axis. As illustrated in Figure 6(b), the distribution of these fracture trace angles predominantly spans a range from -20 degrees to 20 degrees. This range indicates the variation in the orientation of fracture trace relative to the wellbore axis.

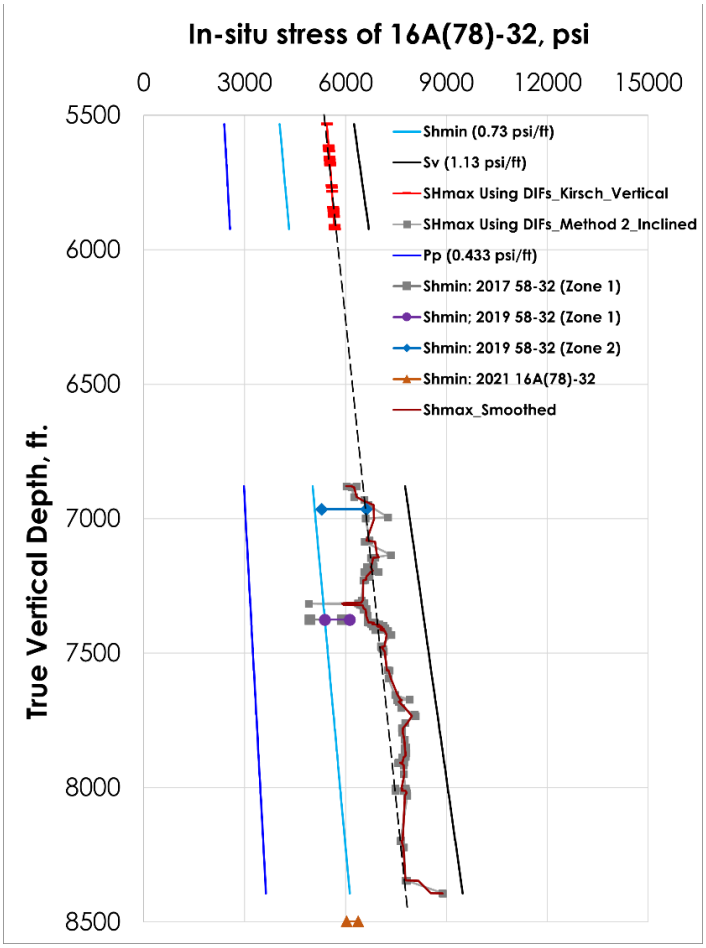

Figure 4: The stress profile of the deviated well 16A(78)-32 using Method 2.

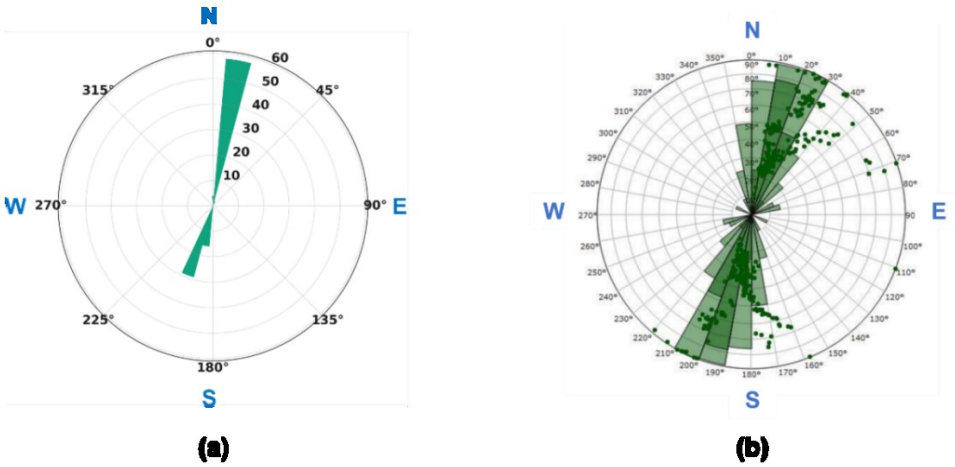

Figure 5: (a) The azimuth of drilling-induced fractures in deviated well 16A(78)-32, inferred from the stress inversion using Method 2, suggests that the orientation of S_{Hmax} ranges from N5°E to N30°E. (b) The azimuth of drilling-induced fractures in deviated well 16A(78)-32, observed from the image logs, suggests that the orientation of S_{Hmax} ranges from N10°E to

N40°E. The inferred results have fewer data points due to the exclusion of image logs from the build-up section and the removal of non-converging inversion results.

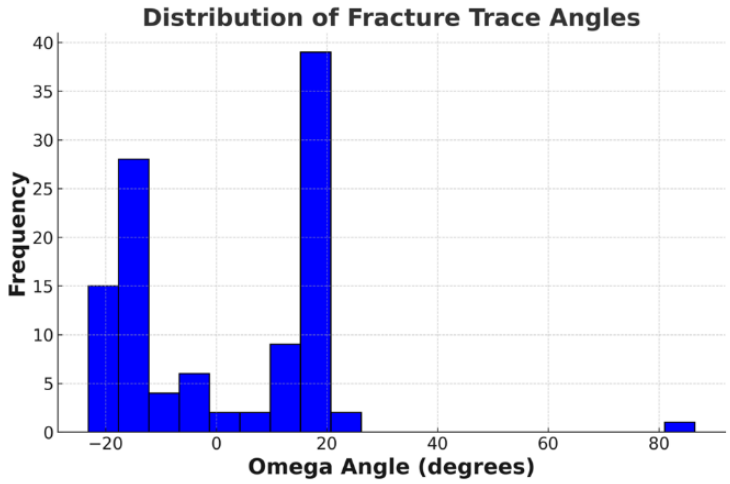

Figure 6: The inferred distribution of the fracture trace angle using Method 2.

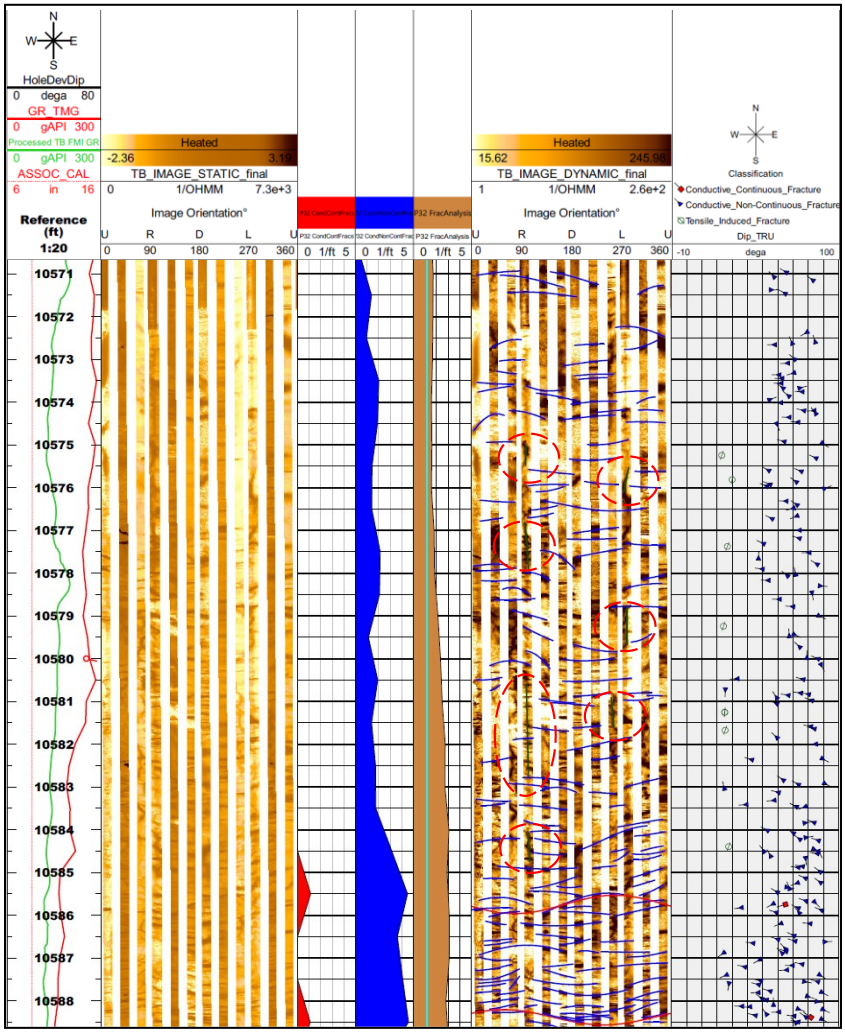

Figure 7: The FMI image logs of FORGE well 16A(78)-32 at the interval of 10571-10588 ft. (or 8,380 – 8,390 ft in true vertical depth) reveal many short, closely-spaced transverse fractures (indicated by the blue, short transverse lines), along with some axial fractures (highlighted by red circles on the axial green lines).

4. ANALYSIS OF TRANSVERSE FRACTURES

In addition to drilling-induced fractures, borehole image logs from the 16A(78)-32 well reveal several zones of closely spaced, short fractures transverse to the wellbore. As demonstrated by Figure 7, in the section near the toe at the interval of 10,571 - 10,588 ft. (or 8,380 – 8,390 ft in true vertical depth), there are small axial fractures and numerous seemingly transverse fractures visible in the FMI image logs. If these fractures are not naturally occurring but are thermally induced due to cooling, they suggest potential tensile failure in the axial direction. Both axial and transverse fractures can be analyzed to determine lower bound for the S_{Hmax}'s magnitude (Ye at al., 2022). The formation of these transverse fractures necessitates that the effective axial stress at certain points along the wellbore wall is tensile and of sufficient magnitude to surpass the tensile strength of the rock (note that if the tangential stress σ_{tt}, or more generally the minimum principal stress, becomes tensile around the wellbore, transverse fractures can form). This requirement is described in the following equation:

$$\sigma_{zz} - \alpha P_p = -T \tag{19}$$

Where σ_{zz} represents the axial stress acting on the borehole in the direction parallel to the borehole trace. It can be calculated using Equation (8). In this study of failure analysis, the Biot's coefficient is set to 1.

Similar to Method 1, we can determine the magnitude of S_{Hmax} by solving Equation (19), assuming all other parameters are known. Figure 8 presents the preliminary S_{Hmax} values deduced from the transverse fractures within the interval of 10,571 - 10,588 ft. (or 8,380 – 8,390 ft in true vertical depth). The findings reveal that the S_{Hmax}'s magnitudes inferred from most transverse fractures (represented by blue dots in Figure 8) are much larger than the vertical stress (S_v), with a minimum gradient observed at 1.25 psi/ft. In contrast, a smaller subset of these fractures, indicated by red dots in Figure 8, suggests S_{Hmax}'s magnitudes lower than S_v. Considering the broader in-situ stress analysis at the Utah FORGE site, which includes the analysis of drilling-induced fractures as shown in the above sections, the prevailing stress regime is expected to be conducive to normal faulting, or possibly strike-slip faulting at greater depths. This implies that the magnitude of S_{Hmax} at FORGE is likely either lower to or slightly greater than S_v. Consequently, the majority of transverse fractures, requiring S_{Hmax} significantly above the anticipated range, are likely natural in origin rather than thermally-induced tensile fractures. This is supported by their requirement for a higher S_{Hmax} for initiation, as shown by the blue dots. However, the presence of some transverse fractures that correspond to a lower S_{Hmax} (as per the red dots in Figure 8) suggests the possibility of them being thermally induced. This analysis aids in discerning the nature of transverse fractures and understanding the subsurface stress state at the FORGE site.

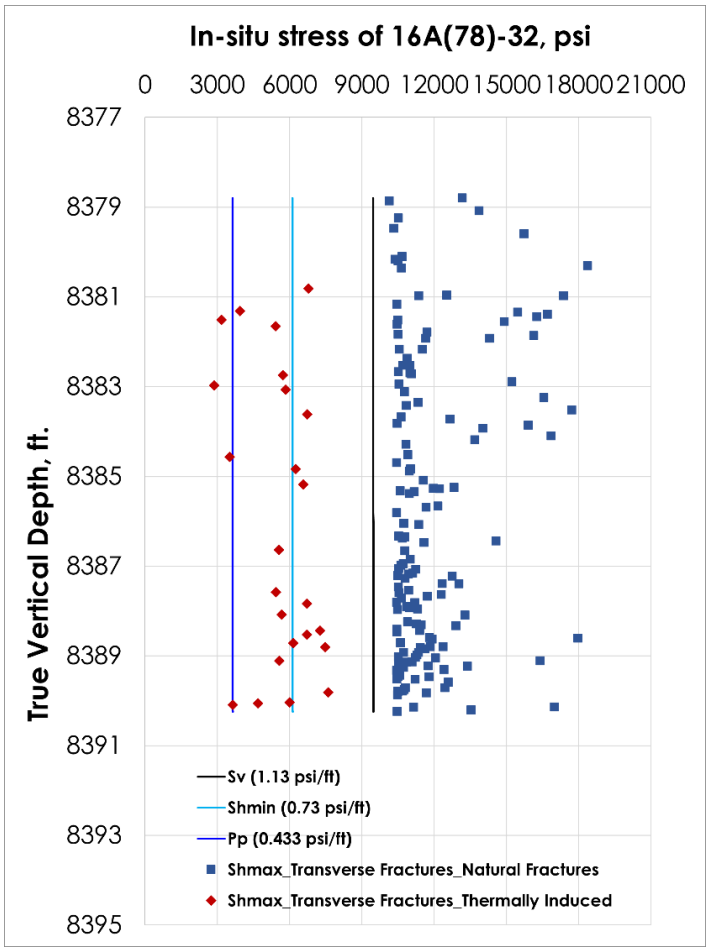

Figure 8: The stress profile for the interval of 10571-10588 ft. (or 8,380 – 8,390 ft in true vertical depth) in well 16A(78)-32. The magnitude of S_{Hmax} was determined by transverse fractures.

In our related study (Ghassemi et al., 2024), we utilized a fully coupled 3D thermo-poroelastic model to examine the origin of the transverse fractures identified in well 16A(78)-32, as depicted in Figure 7. Our findings revealed that the effective axial stress (σ'_{zz}) becomes tensile in a localized area surrounding the wellbore, primarily due to thermal stresses induced by cooling. This results in a tensile failure zone where thermally-induced transverse fractures could start. However, it is important to note that the tensile failure stress zone is limited to a small region. This observation aligns with the analysis in the present study, which suggested that only a minor fraction of these transverse fractures (illustrated by the red dots in Figure 8) might be thermally induced. Moreover, the majority of these transverse fractures remained stable, characterized by their short length and lack of extension across the entire wellbore diameter, as clearly visible in the image logs (Figure 7). This further supports the notion that most of these fractures are naturally occurring rather than a result of thermal stress.

5. CONCLUSIONS

This paper presents a detailed stress analysis and updated wellbore stress models for the Utah FORGE site, specifically focusing on the deviated injection well 16A(78)-32. We have constrained the magnitude of S_{Hmax} by analyzing drilling-induced fractures observed in the image logs of this deviated well. Two methods were applied: Method 1, which determines S_{Hmax} as the only unknown parameter, and Method 2, a more advanced stress inversion technique that considers three unknowns—S_{Hmax}'s magnitude, its orientation, and the fracture trace angle (ω). Method 1 yielded scattered results, indicating that S_{Hmax}'s magnitude is approximately 0.88-1.37 psi/ft, suggesting possible strike-slip faulting in deeper formations. In contrast, Method 2 appears to provide more reliable stress results, with S_{Hmax} constrained to a range of 0.87-1.06 psi/ft, indicative of a normal to potentially transitional faulting regime. The orientation of S_{Hmax}, as deduced by Method 2, varies from N5°E to N30°E, closely aligning with the orientation indicated by drilling-induced fractures, thereby enhancing the reliability of our stress analysis. Additionally, we analyzed a section near the toe of well 16A(78)-32, characterized by numerous short, closely-spaced transverse fractures visible in the image logs. Our stress analysis suggests the presence of thermally-induced transverse fractures due to tensile failure. However, it appears that the majority of these transverse fractures are of natural origin, with only a small portion being thermally-induced by cooling during drilling activities. This interpretation aligns with our related study (Ghassemi et al., 2024), which employed fully coupled 3D thermo-poroelastic modeling to investigate the origins of these transverse fractures. The simulation results indicated a limited zone of tensile failure around the wellbore due to thermal stress from cooling, suggesting that only a limited number of transverse fractures could be thermally induced. These updated wellbore stress models and analytical techniques provide a more accurate understanding of in-situ stress at the Utah FORGE site, which is critical for optimizing drilling operations, hydraulic stimulation processes, and mitigating induced seismicity in EGS development. It should be added that focal mechanism interpretations of microseismicity from Stage 3 stimulation indicate strike-slip and reverse faulting regime events. The nature of the events is currently under investigation as part of the Utah FORGE R&D project OU-2-2404.

ACKNOWLEDGEMENTS

This project was supported by the Utah FORGE project sponsored by the U.S. Department of Energy, through the project "Application of Advanced Techniques for Determination of Reservoir-Scale Stress State at Utah FORGE."

REFERENCES

Aadnoy, B. S., and Bell, J. S.: Classification of Drilling-induced Fractures And Their Relationship To In-situ Stress Directions. The Log Analyst, 1998, 39(06).

Aadnoy, B. S., and Chenevert, M. E.: Stability of highly inclined boreholes. SPE drilling engineering, 2(04), (1987), 364-374.

Aadnoy, B. S.: In-situ stress directions from borehole fracture traces. Journal of Petroleum Science and Engineering, 4(2), (1990), 143-153.

Bell, J. S. and Gough, D. I.: The use of borehole breakouts in the study of crustal stress. Hydraulic fracturing stress measurements, (1983), 201-209.

Brody, M., and Kjorholt, H.: The initiation of drilling-induced tensile fractures and their use for the estimation of stress magnitude. Proceedings, Vail Rocks 1999, 37th US Symposium on Rock Mechanics (1999).

Fang, Y., Ye, Z., and Ghassemi, A.: Preliminary Wellbore In-situ Stress Models for Utah FORGE. Proceedings, 2022 Geothermal Rising Conference (GRC), Reno, Nevada, USA (2022)..

Ghassemi, A., Ye, Z., and Ratnayake, M.: The Role of thermo-poroelastic Effects on Drilling Induced Fractures in the Utah FORGE Well 16A(78)-32. Proceedings, 49th Workshop on Geothermal Reservoir Engineering, Stanford, California (2024).

Huang, J., Griffiths, D. V., and Wong, S. W.: In situ stress determination from inversion of hydraulic fracturing data. International Journal of Rock Mechanics and Mining Sciences, 48(3), (2011), 476-481.

Okabe, T., Hayashi, K., Shinohara, N., and Takasugi, S.: Inversion of drilling-induced tensile fracture data obtained from a single inclined borehole. International Journal of Rock Mechanics and Mining Sciences, 35(6), (1998), 747-758.

Peška, P., and Zoback, M. D.: Compressive and tensile failure of inclined well bores and determination of in situ stress and rock strength. Journal of Geophysical Research: Solid Earth, 100(B7), (1995), 12791-12811.

Schmitt, D. R., and Zoback, M. D.: Poroelastic effects in the determination of the maximum horizontal principal stress in hydraulic fracturing tests—a proposed breakdown equation employing a modified effective stress relation for tensile failure. International Journal of Rock Mechanics and Mining Sciences & Geomechanics Abstracts, 26(6), (1989), 499-506.

Thorsen, K.: In situ stress estimation using borehole failures—Even for inclined stress tensor. Journal of Petroleum Science and Engineering, 79(3-4), (2011), 86-100.

Ye, Z., Fang, Y., Ghassemi, A., and McLennan, J.: A Preliminary Wellbore In-Situ Stress Model for Utah FORGE. Proceedings, ARMA US Rock Mechanics/Geomechanics Symposium, Santa Fe, New Mexico (2022)

Zoback, M. D., and Haimson, B. C.: Status of the hydraulic fracturing method for in-situ stress measurements. Proceedings, the 23rd US Symposium on Rock Mechanics (USRMS), Berkeley, California (1982).